

## MODELING STATIC MAGNETIC FIELD STRUCTURES IN SOLAR CORONA

V. M. Čadež

*Astronomical Observatory, Volgina 7, 11160 Belgrade 74, Serbia and Montenegro*

(Received: November 4, 2005; Accepted: November 4, 2005)

**SUMMARY:** We give an overview of procedures to recover and simulate typical coronal static magnetic field topologies from given boundary data on the photosphere. Relatively simple analytical treatments allow for solutions representing magnetic structures that are invariant in one coordinate, and satisfying prescribed boundary conditions. Starting from elementary active regions in a form of localized sources/sinks of magnetic field lines on the photospheric level, we set up various composed boundary conditions which yield complex magnetic structures in the corona above.

**Key words.** Sun: magnetic fields – Sun: corona

### 1. INTRODUCTION

Numerous observations of the solar corona performed in particular spectral lines of X-ray and EUV emission show that its temporal and spatial structures are dominated by the magnetic field emerging through the photosphere and expanding out into the corona and further into the interplanetary space and the entire heliosphere. Such observed coronal structures, however, provide no information on magnetic field strength which makes the determination of magnetic field topologies in the corona a primary step in a process of understanding the physics of coronal features and phenomena such as flares and coronal mass ejections. Unfortunately, direct observations and measurements of coronal magnetic fields are very difficult, practically impossible, at least at the level and capabilities of existing observational methodologies based on Zeeman spectral line splitting and on characteristics of light polarization induced by the ambient magnetic field the observed radiation is normally passing through. The main difficulties arise from a very high coronal temperature which broadens spectral lines orders of magnitude above the Zeeman splitting, and from

the fact that coronal lines are optically thin which makes them difficult for interpretation (Wiegmann et al. 2005). Another possibility to estimate intensities of coronal local magnetic fields is by the gyroresonance radio emission in centimeter wavelength emitted from active regions on the Sun which is a developing techniques yet far from being sufficient and fully reliable.

On the other hand, the photospheric and also chromospheric magnetic fields are much easier to measure. The contemporary vector magnetographs provide sufficient data on the linear and circular polarization of light to recover all three magnetic vector components on the photosphere. These photospheric magnetic field distributions are now used as boundary conditions in computations of adjacent coronal magnetic field topologies and their comparisons with shapes of optically observed structures such as magnetic arcades, loops, streamers, canopies etc. However, this problem of extrapolation of photospheric magnetic fields into the corona is neither simple nor straightforward as we do not know which type of magnetic field we are really dealing with, i.e. which equations we have to solve. Then, does the boundary condition of the magnetic field on the photosphere

suffice for a unique solution in the corona with a proper asymptotic behaviour at infinity? What are contributions of electric currents in the corona to its magnetic field distribution? Such questions cannot be answered in a simple way which leaves the door open to approximations and a priori assumptions in making physical models of the system photosphere-corona to compute coronal magnetic fields. Thus, Petrie and Neukirch (2000) use the Green's function method for a class of 3D magnetohydrostatic equilibria arising from a combination of force-free and non force-free electric currents while Yan and Sakurai (2000) and Yan (2003) are utilising a different method of solving a boundary integral equation numerically. Amari et al. (1999) included additional shear and twist of magnetic field lines in their computational modeling of coronal fields, Lee et al. (1999) use also data from radio observations for a better estimate of the nature of coronal magnetic fields. Wang et al. (2000) developed a numerical technique to study developments and evolutions of particular magnetic field structures in the corona such as quasi-separatrix layers where magnetic reconnections can take place and promote chromospheric and coronal heating. Similarly, Yiao et al. (1997) recovered the coronal magnetic field over an active region in the force-free approximation. Various numerical methods involving Legendre polynomial expansions, solar wind simulations and corrections of magnetograph data due to saturation were discussed a long time ago by Altschuler and Newkirk (1969).

Magnetic fields of the solar corona have generally very complex structure depending on the solar activity cycle. Often, however, they take shapes of arcades and loops emerging from the photosphere, penetrating through the coronal medium and sinking into the photosphere again. Observational data indicate large spatial scales of such magnetic structures and their stationarity over comparatively long time intervals. In this paper, we derive and analyze analytical expressions that can be used for modeling coronal magnetic fields if the magnetic field potential, also known as the flux function, is initially given on the photospheric plane (Lothian and Browning 1995). Such a boundary condition can, in principle, be related to observational data (Sakurai 1989, Yan and Wang 1995).

The paper is organized as follows: an introduction into the coronal magnetic field computations is given in Chapter 1, a magneto-hydrostatic (MHS) equilibrium assuming invariance in one coordinate in the Cartesian geometry is discussed in Chapter 2 while Chapter 3 deals with low plasma  $\beta$ , or force-free, magnetic field configurations. Chapter 4 contains examples of complex potential magnetic field configurations resulting from combinations of individual localized active regions, Chapter 5 tackles the problem of derivation of 3D force-free coronal magnetic fields from magnetic vector data on the photosphere, and some conclusion and remarks are found in Chapter 6.

## 2. STATIC EQUILIBRIUM - 2.5D CARTESIAN GEOMETRY

MHS equilibria are practically impossible to be treated analytically in general 3D configurations due to insurmountable mathematical difficulties. In such cases, only lengthy numerical procedures involving various computational techniques can yield satisfactory results. However, to obtain a better insight into the background physics of the problem and to understand its governing processes it is desirable to handle the problem also by some analytical means. This usually requires introduction of certain simplifications to make mathematical analyses doable but then a care has to be taken about limitations in applicability of results obtained in such a way.

In this sense, we shall simplify the model of a general magneto-hydrostatic equilibrium by assuming its spatial dependence to be 2D, say dependent on two variables  $x$  and  $z$  taken in the horizontal and vertical direction respectively. At the same time, the magnetic field may have all three components, i.e. it is treated in 3D. Consequently, such a basic state configuration is  $y$ -invariant and can be looked at as a 2.5 dimensional structure. This approach (Edenstrasser 1980) allows us to introduce numerous analytically obtained magnetic field structures that can be relevant in modeling observational features commonly seen in the solar corona.

The equilibrium of the considered  $y$ -invariant ( $\partial/\partial y = 0$ ) basic state is described by the MHS equation:

$$\frac{1}{\mu_0}(\nabla \times \vec{B}) \times \vec{B} - \nabla p - \rho g \nabla z = 0 \quad (1)$$

where  $\mu_0 = 4\pi 10^{-7}$  H/m is the magnetic permeability of free space.

The magnetic field  $\vec{B} \equiv (B_x, B_y, B_z)$  can be split into two components, the perpendicular and the parallel, with respect to the  $y$ -axis of invariance:

$$\vec{B} = \vec{B}_\perp + B_y \hat{e}_y \quad \text{and} \quad \vec{B}_\perp \equiv (B_x, 0, B_z). \quad (2)$$

The perpendicular component  $\vec{B}_\perp(x, z)$  can further be expressed in terms of the related magnetic vector potential  $\vec{A} \equiv (0, A(x, z), 0)$  as:

$$\vec{B}_\perp = \nabla \times \vec{A} = \nabla A \times \hat{e}_y \quad (3)$$

implying

$$\vec{B}_\perp \cdot \nabla A = 0 \quad (4)$$

or  $A = \text{const.}$  along the field lines of the perpendicular magnetic field  $\vec{B}_\perp$ . In other words, these field lines are curves whose analytical expressions are  $A(x, z) = \text{const.}$

Considering the expressions (2) and (3), the MHS condition (1) takes the following form:

$$\begin{aligned} &(\vec{B}_\perp \cdot \nabla B_y) \hat{e}_y - B_y \nabla B_y - (\nabla^2 A) \nabla A \\ &- \mu_0 \nabla p - \mu_0 \rho g \nabla z = 0 \end{aligned} \quad (5)$$

or, in components taken along and perpendicular to the y-axis respectively:

$$\vec{B}_\perp \cdot \nabla B_y = 0, \quad (6)$$

$$\mu_0 \nabla p = -B_y \nabla B_y - (\nabla^2 A) \nabla A - \mu_0 \rho g \nabla z \quad (7)$$

Substituting Eq. (3) into Eq. (6) one gets:

$$(\nabla A \times \nabla B_y) \cdot \hat{e}_y = 0. \quad (8)$$

Since  $\hat{e}_y \cdot \nabla A = 0$  and  $\hat{e}_y \cdot \nabla B_y = 0$  according to the assumed y-invariance, the above relation (8) requires  $\nabla A \times \nabla B_y = 0$  indicating the collinearity of vectors  $\nabla A$  and  $\nabla B_y$  meaning that:

$$\nabla B_y = \frac{dB_y}{dA} \nabla A \quad \text{i.e.} \quad B_y = B_y(A) \equiv \mathcal{F}_y(A). \quad (9)$$

The magnetic field component  $B_y$  is therefore an arbitrary function  $\mathcal{F}_y$  of only one variable  $A$ , and has to be prescribed as the initial condition. As pointed out, the quantity  $A = A(x, z)$  defines field lines  $A = \text{const.}$  of  $\vec{B}_\perp$  in the  $(x, z)$ -coordinate plane if viewed in 2D. Looking in 3D and taking the  $y$ -invariance into account, the relation  $A(x, z) = \text{const.}$  represents cylindrical surfaces along the  $y$ -axis while the field lines of  $\vec{B}_\perp$  are cross-sections of cylindrical surfaces  $A(x, z) = \text{const.}$  and planes  $y = \text{const.}$  The property  $B_y = \mathcal{F}_y(A)$  further implies that a fixed magnetic field component  $B_y$  has to be added to the field  $\vec{B}_\perp$  along its field lines on the cylindrical surface  $A(x, z) = \text{const.}$  to obtain the total magnetic field  $\vec{B}$ . The resulting field lines of  $\vec{B}$  remain therefore on cylindrical surfaces  $A = \text{const.}$  but they are not sections with the  $y = \text{const.}$  planes anymore. They are sheared by the amount of the added magnetic field component  $B_y = \mathcal{F}_y(A)$ .

Now, Eq. (7) becomes:

$$\nabla p = -\frac{1}{\mu_0} \left( \nabla^2 A + \frac{d}{dA} \frac{\mathcal{F}_y^2}{2} \right) \nabla A - \rho g \nabla z. \quad (10)$$

Thus, the spatial distribution of the pressure field  $p(x, z)$  is given by  $p = p(A, z)$  and one can write the following expression for the pressure gradient:

$$\nabla p = \frac{\partial p}{\partial A} \nabla A + \frac{\partial p}{\partial z} \nabla z. \quad (11)$$

A comparison of the two expressions for  $\nabla p$ , i.e. Eqs. (10) and (11), yields:

$$\frac{\partial p}{\partial A} = -\frac{1}{\mu_0} \left( \nabla^2 A + \frac{d}{dA} \frac{\mathcal{F}_y^2}{2} \right), \quad (12)$$

$$\frac{\partial p}{\partial z} = -\rho g. \quad (13)$$

Eq. (13) can easily be integrated over the variable  $z$  if the considered plasma is assumed to obey the perfect gas law  $p = \rho \mathcal{R}T$  ( $\mathcal{R}$  is the individual gas constant for a specific gas composition) and if the temperature profile  $T(x, z)$  is a known function initially prescribed. Taking the simplest example of a uniform temperature  $T \equiv T_0 = \text{const.}$ , we get from Eq. (13):

$$p \equiv p(A, z) = p_0(A) e^{(-z/H)} \quad (14)$$

where  $p_0(A)$  is the boundary value for the pressure distribution on magnetic field lines  $A(x, z) = \text{const.}$  at  $z = 0$  and  $H \equiv \mathcal{R}T_0/g$ . Inserting Eq. (14) for  $p(A, z)$  into Eq. (12) we obtain the final equation for the potential  $A = A(x, z)$ :

$$\nabla^2 A + \frac{d}{dA} \left[ \frac{\mathcal{F}_y^2(A)}{2} + \mu_0 p_0(A) e^{(-z/H)} \right] = 0. \quad (15)$$

As one can see, Eq. (15) contains two quantities  $\mathcal{F}_y(A)$  and  $p_0(A)$  that we are free to specify according to needs of the model under consideration. Once the solution of Eq. (15) for  $A(x, z)$  is obtained, we readily derive the final expressions for the total magnetic field  $\vec{B}(x, z)$  from Eqs. (2) and (3) as:

$$\begin{aligned} B_x(x, z) &= -\frac{\partial A}{\partial z}, \\ B_y(x, z) &= \mathcal{F}_y(A), \\ B_z(x, z) &= \frac{\partial A}{\partial x}, \end{aligned} \quad (16)$$

and the pressure  $p(A, z)$  from Eq. (14). As for the density  $\rho$ , it follows from the perfect gas law:  $\rho(A, z) = p(A, z)/\mathcal{R}T_0$  with  $T_0$  assumed uniform in this particular example.

### 3. LOW PLASMA – $\beta$ MAGNETIC FIELD CONFIGURATIONS IN 2.5D

Many coronal magnetic field structures which remain in quasi-static equilibria over comparatively long time spans have also a typical property of being characterized by very large magnetic Reynolds numbers  $R_m$  ( $10^{10}$  and more) arising mostly from extremely high electrical conductivity  $\sigma$  of the coronal plasma (typically  $\sigma \sim 10^6$  S/m) and large geometrical length-scales of magnetic structures (typical sizes  $L \sim 10^7$  m). In such cases, the effects of magnetic diffusivity become negligible within the life-time of a magnetic structure. Furthermore, the thermal pressure  $p$  of the coronal plasma is generally found much smaller than the corresponding magnetic pressure

$p_m \sim B^2$  which allows for the low plasma- $\beta$  approximation to be applied which significantly simplifies analytical treatments. Namely, if  $1 \gg \beta \equiv p/p_m$  the magnetic forces dominate both the thermal pressure gradient force and gravity force meaning that condition (1) for the total MHS balance is practically satisfied by the equilibrium of magnetic forces only and Eq. (1) reduces to a much simpler expression

$$(\nabla \times \vec{B}) \times \vec{B} \approx 0 \quad (17)$$

for a force-free magnetic field. Such force-free magnetic fields are widely utilised in modelings of coronal field structures (Levine and Altschuler 1974, Aly and Seehafer 1993). In this case, Eq. (15) for  $A$  reduces to a Grad-Shafranov type of equation:

$$\nabla^2 A + \frac{d}{dA} \left[ \frac{\mathcal{F}_y^2(A)}{2} \right] = 0 \quad (18)$$

if the  $y$ -invariance is assumed.

Eq. (17) for a force-free magnetic field indicates the alignment of  $\vec{B}$  with the current  $\vec{j} = \nabla \times \vec{B}/\mu_0$  which can be written as

$$\nabla \times \vec{B} = \alpha \vec{B} \quad (19)$$

where the proportionality factor  $\alpha$  is some scalar function of spatial coordinates. The physical significance of  $\alpha$  can easily be seen if the expressions (2) and (3) are substituted into Eq. (19) whose  $y$ -component then reduces to:

$$\alpha = \frac{d\mathcal{F}_y}{dA} \equiv \frac{dB_y(A)}{dA} \quad (20)$$

with Eq. (18) taken into account. The obtained relation (20) indicates  $\alpha = \alpha(A)$ , i.e. that  $\alpha$  too is constant along the field-lines of the total magnetic field as they are laying on cylindrical surfaces  $A(x, z) = \text{const}$ . Also,  $\alpha$  is not an arbitrary function, it is determined by the choice of  $B_y = B_y(A)$ .

Eq. (20) shows that the force-free magnetic fields given by Eq. (19) have all three components different from zero with  $B_y \neq \text{const}$ . if  $\alpha \neq 0$ . In a special case of  $\alpha = 0$ , corresponding to the well known class of current-free or potential magnetic fields, the magnetic field component  $B_y$  is constant in space:  $B_y = c_0 = \text{const}$ .

To obtain the magnetic field components Eq. (16), we have to solve Eq. (18) for  $A(x, z)$  with prescribed boundary conditions at the  $z = 0$  plane. This equation is evidently nonlinear due to the term  $\mathcal{F}_y(A)$  and it cannot be solved analytically in its general form. However, there exist some special possibilities allowing for instructive analytical solutions that can easily be derived for different types of magnetic field. Thus, choosing:

$$\begin{aligned} \mathcal{F}_y(A) &= c_0 & \implies \alpha &= 0, \\ \mathcal{F}_y(A) &= c_1 A & \implies \alpha &= c_1, \\ \mathcal{F}_y(A) &= c_2 A^2 & \implies \alpha &= 2c_2 A, \end{aligned} \quad (21)$$

one obtains a potential magnetic field, a linear, and nonlinear non potential force-free field respectively. Here,  $c_{0,1,2}$  are constants to be defined according to requirements of the considered model.

In what follows, we are going to study potential magnetic field configurations in more details and show the results for some typical examples of boundary conditions.

#### 4. POTENTIAL MAGNETIC FIELD CONFIGURATIONS IN 2D

As already mentioned, a potential magnetic field is current-free meaning that  $\alpha = 0$  in Eq. (19). The  $B_y$  component of  $\vec{B}$  is then constant equal to  $c_0$  as indicated by Eqs. (20)-(21). To simplify the problem without loosing much of its generality, we shall take  $B_y = 0$  which makes the magnetic field topology 2D with two magnetic field components  $B_x$  and  $B_z$ , and magnetic field lines in the  $(x, z)$ -plane given by the family of curves  $A(x, z) = \text{const}$  (Oliver et al. 1999). Such 2D curves represent cylindrical surfaces of equal normal cross-section in the  $y$ -direction if viewed in 3D which makes them suitable for modeling magnetic arcade structures often existing in the solar corona. The potential  $A$ , also known as the flux function, is the solution of Eq. (18) with prescribed boundary conditions.

##### 4.1 General analytical solution

Taking  $B_y = 0$  in Eq. (18), we obtain the Laplace equation

$$\frac{\partial^2 A(x, z)}{\partial x^2} + \frac{\partial^2 A(x, z)}{\partial z^2} = 0 \quad (22)$$

to be solved with boundary conditions that:

1. Prescribe the distribution of  $A$  along the horizontal  $x$ -axis at the  $z = 0$  level (the photosphere). Thus,  $A_0(x) \equiv A(x, 0)$  is a prescribed known function of  $x$  defined as to describe some realistic distribution of the magnetic field, more precisely its vertical  $z$ -component at  $z = 0$ . Namely, the boundary value of the flux function  $A_0(x)$  and  $B_z(x, 0)$  are mutually related as seen in Eq. (16).
2. Provide physically acceptable solutions with magnetic field amplitude (and the energy) falling off with height  $z$ .

Now, Eq. (22) can first be Fourier transformed in the horizontal variable  $x$  which gives an ordinary second order differential equation

$$\frac{d^2 A_k(z)}{dz^2} - k^2 A_k(z) = 0. \quad (23)$$

where:

$$A_k(z) = \frac{1}{\sqrt{2\pi}} \int_{-\infty}^{+\infty} A(x, z) e^{-ikx} dx \quad (24)$$

is the Fourier transform of  $A(x, z)$ .

Next, the solution of Eq. (23) satisfying the described boundary conditions is readily obtained as:

$$A_k(z) = A_k(0) e^{-kz} \quad (25)$$

where  $A_k(0)$  is the Fourier transform of the prescribed boundary condition  $A(x, 0) \equiv A_0(x)$  or, according to Eq. (24),

$$A_k(0) = \frac{1}{\sqrt{2\pi}} \int_{-\infty}^{+\infty} A_0(x) e^{-ikx} dx. \quad (26)$$

Finally, after performing the inverse Fourier transform to  $A_k(z)$  in Eq. (25), the solution of Eq. (22) for the flux function  $A(x, z)$  which satisfies the prescribed boundary conditions becomes:

$$A(x, z) = \frac{1}{\sqrt{2\pi}} \int_{-\infty}^{+\infty} A_k(z) e^{ikx} dk \quad (27)$$

or

$$A(x, z) = \frac{1}{\sqrt{2\pi}} \int_{-\infty}^{+\infty} A_k(0) e^{(ix-z)k} dk. \quad (28)$$

The topology of the 2D potential magnetic field in the corona (the region  $z > 0$ ) emerging from the boundary conditions at  $z = 0$  (the photosphere) is now depicted by the family of curves  $A(x, z) = \text{const.}$  while the magnetic field components follow from Eq. (16).

## 4.2 Boundary conditions for models of active regions

The boundary condition given through the functional dependence  $A_0(x)$  can be used to model 2D magnetic active regions on the surface of the photosphere at  $z = 0$ . We start from the simplest case of a 'unipolar active region' defined as a domain with locally enhanced concentration of the vertical component of magnetic field with the same orientation, i.e. a localized 'source/sink' of magnetic field lines at  $z = 0$ . The 'strength' of such an active region will be taken proportional to the local flux density of magnetic field lines, and its sign determined depending on whether the magnetic field lines are emerging from the photosphere into the corona (a 'source') when the sign is positive, or they are sinking from the corona into the photosphere (a 'sink') when the sign is negative. According to Eq. (16), the normal component of magnetic field at  $z = 0$  is given by

$$B_z(x, 0) = \frac{dA_0(x)}{dx}$$

meaning that an active region with enhanced  $B_z(x, 0)$  is characterized by a large  $x$ -derivative of  $A_0(x)$ .

A single unipolar active region is now modeled by a functional dependence  $A_0(x)$  appropriately chosen as to exhibit a localized domain with a steep gradient and a relatively uniform behaviour elsewhere. To describe a single active region located around  $x = x_0$ , we use the following functional dependence for the boundary condition  $A_0(x)$ :

$$A_0(x) = a_0 \tanh\left(\frac{x - x_0}{L}\right) \quad (29)$$

which is related to the vertical magnetic field component

$$B_z(x, 0) = \frac{a_0}{L} \cosh^{-2}\left(\frac{x - x_0}{L}\right). \quad (30)$$

The magnitude and sign of the coefficient  $a_0$  thus determine the strength and type (source/sink) of a unipolar active region respectively while  $L$  defines its linear extent around  $x = x_0$ .

Having defined the boundary condition Eq. (29) for a unipolar active region, we obtain its Fourier transform

$$A_k(0) = -i \left(\frac{\pi}{2}\right)^{-1/2} \frac{a_0 L}{\sinh\left(\frac{\pi}{2} k L\right)} e^{ikx_0} \quad (31)$$

from Eq. (26) and then the final solution:

$$A(x, z) = a_0 L \int_0^{+\infty} \frac{\sin[k(x - x_0)]}{\sinh\left(\frac{\pi}{2} k L\right)} e^{-kz} dk \quad (32)$$

from Eq. (27).

Once a model for an elementary single active region is resolved by choosing the boundary condition Eq. (29) for the flux-function, one can model a complex structure composed of  $N$  different single active regions by solving the linear equation (22) with a boundary condition given by a linear combination of boundary conditions (29) for each of  $N$  single active regions:

$$A_0(x) = \sum_{n=1}^N a_0^{(n)} \tanh\left[\frac{x - x_0^{(n)}}{L^{(n)}}\right]. \quad (33)$$

Thus, for example, a symmetric dipole active region occurs for  $N = 2$  and  $a_0^{(1)} = -a_0^{(2)}$  while numerous other combinations yield interesting magnetic field topologies in the corona  $z \geq 0$ . Some of them are suitable for modeling magnetic fields supporting prominences, like those with local depressions-minima, some take forms of coronal hole structures with open magnetic field lines, etc.

The resulting flux-function  $A(x, z)$  which follows from Eq. (28) with the boundary condition (33) is then a superposition of solutions (32):

$$A(x, z) = \sum_{n=1}^N a_0^{(n)} L^{(n)} \int_0^{+\infty} \frac{\sin[k(x - x_0^{(n)})]}{\sinh\left(\frac{\pi}{2} k L^{(n)}\right)} e^{-kz} dk. \quad (34)$$

So far, we were interested in coronal magnetic fields from localized active regions on the photosphere whose topology is given by  $A(x, z) = \text{const}$ . However, we can also assume the existence of some additional solar global potential magnetic fields superimposed on those from localized sources/sinks, and which may be taken locally uniform, i.e. planar. In this case, the flux-function  $A^{(g)}(x, z)$  for such a global magnetic field  $\vec{B}^{(g)}$  is clearly

$$A^{(g)}(x, z) = B_z^{(g)}x - B_x^{(g)}z \quad (35)$$

as seen from expressions in Eq. (16). The total magnetic field topology then follows from Eqs. (34)-(35) as:

$$A^{(\text{tot})}(x, z) \equiv A^{(g)}(x, z) + A(x, z) = \text{const.} \quad (36)$$

Some typical examples of magnetic field configurations  $A = \text{const}$  with  $A$  given by Eq. (34) are shown in Fig. 1 for four different numbers  $N$  of localized sources at  $z = 0$ , and in absence of a global magnetic field (i.e. with  $\vec{B}^{(g)} = 0$ ).

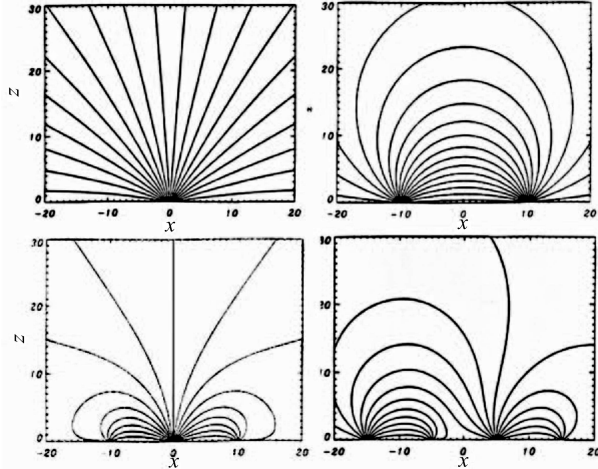


**Fig. 1.** Examples of magnetic field topologies generated by  $N=1, 2, 3$  and  $4$  localized active regions -sources/sinks- at  $z = 0$ .

The corresponding coefficients  $a_0^{(n)}$  and  $L^{(n)}$  in Fig. 1 have the following values:

$N = 1$ , one active region:

$$a_0^{(1)} = 1, L^{(1)} = 1.$$

$N = 2$ , two active regions:

$$a_0^{(1)} = -1, a_0^{(2)} = 1, L^{(1)} = L^{(2)} = 1.$$

$N = 3$ , three active regions:

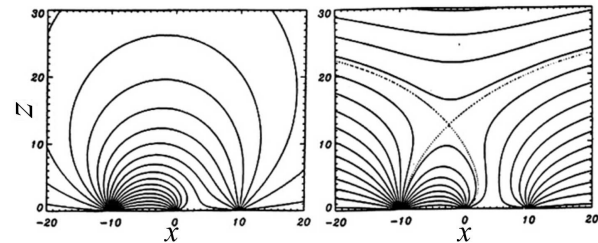
$$a_0^{(1)} = -1, a_0^{(2)} = -3, a_0^{(3)} = 1, L^{(1)} = L^{(2)} = L^{(3)} = 0.3.$$

$N = 4$ , three active regions:

$$a_0^{(1)} = -2, a_0^{(2)} = -1, a_0^{(3)} = -2, a_0^{(4)} = 1, L^{(1)} = L^{(2)} = L^{(3)} = L^{(4)} = 0.3.$$

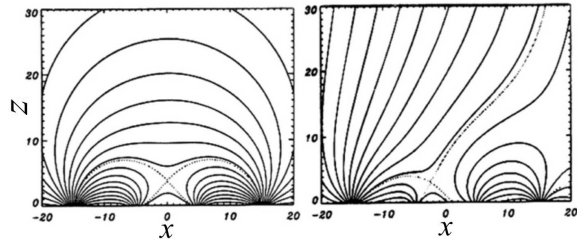
If a global magnetic field  $\vec{B}^{(g)}$  has been present when localized active regions composed of sources/sinks are formed at  $z = 0$ , the resulting field topologies can be quite different from those when  $\vec{B}^{(g)} = 0$ , as seen in Figs. 2-3.

Fig. 2 shows an example with  $N = 3$  localized sources/sinks, with  $a_0^{(1)} = -2, a_0^{(2)} = 1, a_0^{(3)} = 1, L^{(1)} = L^{(2)} = L^{(3)} = 0.3$ , without (left) and with (right) a global horizontal magnetic field  $\vec{B}^{(g)} = (0.08, 0, 0)$ . The corresponding magnetic field topologies follow from Eq. (36) as curves  $A^{(\text{tot})}(x, z) = \text{const.}$



**Fig. 2.** Example of effects caused by a horizontal global magnetic field on magnetic field topology of three localized sources/sinks:  $\vec{B}^{(g)} = 0$  (left), and  $B_x^{(g)} = 0.08$  (right).

We see that the presence of a horizontal global magnetic field, typically found at lower latitudes near the Solar equator, can modify the field topology of three localized active regions in such a way that local minima appear, which is a typical field configuration where prominences can form for example.



**Fig. 3.** Example of effects caused by a vertical global magnetic field on magnetic field topology of four localized sources/sinks:  $\vec{B}^{(g)} = 0$  (left), and  $B_z^{(g)} = 0.08$  (right).

In a similar way, Fig. 3 shows an example of  $N = 4$  localized sources/sinks, with  $a_0^{(1)} = 2, a_0^{(2)} = -1, a_0^{(3)} = 1, a_0^{(4)} = -2, L^{(1)} = L^{(2)} = L^{(3)} = L^{(4)} = 1$ , without (left) and with (right) a global vertical magnetic field  $\vec{B}^{(g)} = (0, 0, 0.08)$ . The assumed vertical global magnetic field, typically found at higher latitudes of Solar polar regions, clearly alters the field topology of four localized active regions

in such a way that a broader domain of open field lines appears which is typical for coronal holes and streamers, for example.

These were just a few illustrations out of countless other possibilities for modeling 2D and  $y$ -invariant magnetic field structures depending on the choice of free parameters  $N$ ,  $a_0^{(n)}$ ,  $L^{(n)}$ ,  $x_0^{(n)}$ ,  $B_x^{(g)}$  and  $B_z^{(g)}$  in Eqs. (34)-(35).

### 4.3 Remarks

The described simplified analytical treatments although performed with approximations, provide a practical insight into how various magnetic field features can result from combinations of localized active regions submerged into a locally uniform global magnetic field. In this way, one can obtain field topologies that resemble those observed in the vicinity of prominences, coronal streamers, neutral-field lines, etc. If viewed in 3D, such  $y$ -invariant 2D solutions become magnetic arcades oriented along the  $y$ -axis. Even if a 2.5D case is considered with  $B_y(A) \neq 0$  added, the shape of such arcades remains unchanged as the resulting magnetic field lines of each arcade are only sheared by a constant amount if  $B_y$  is present.

The considered Cartesian geometry can easily be replaced by other orthogonal coordinate systems provided they allow for invariance in one of its coordinates. For example, in the cylindrical geometry with coordinates  $\rho$ ,  $\phi$  and  $z$ , we can model two types of magnetic arcades: the  $\phi$ -invariant (axially symmetric), and  $z$ -invariant (Čadež et al. 1994, Čadež et al. 2005). The  $r$ -invariance is not possible in cylindrical coordinates due to the intrinsic  $r$ -dependence of some terms in the operator  $\nabla$  in initial equations for magnetic field. Similarly, the spherical geometry allows only for the  $\phi$ - (azimuthal) invariance as  $\nabla$  contains terms depending on  $r$  and  $\theta$  in spherical coordinates. More detailed analyses of non Cartesian geometries including those in generalized orthogonal coordinates  $x_1(x, y, z)$ ,  $x_2(x, y, z)$  and  $x_3(x, y, z)$  are given in Čadež (1996).

## 5. GENERAL FORCE-FREE MAGNETIC FIELD IN 3D SPHERICAL GEOMETRY

So far, we were discussing analytical models of complex 2D active regions composed of localized elementary magnetic sources/sinks on the photospheric boundary  $z = 0$ . The obtained potential magnetic field topologies are invariant in coordinate  $y$  and form cylindrical surfaces, arcades, along the  $y$ -axes. Now we shall treat briefly a generalized case of a force-free magnetic field given by Eq. (19), if the assumption of its invariance in one coordinate is given up. This implies that the coefficient  $\alpha$  is not a function of only one variable  $A$  anymore. Instead, it depends on all three spatial variables, i.e.  $\alpha = \alpha(r, \theta, \phi)$  if the spherical geometry is applied.

As to the boundary condition, one takes the observational data obtained by a vector magnetograph which provides with spatial distributions of all three magnetic field components over a selected area on the surface of the photosphere at  $r = R_\odot$ . However, in spite of knowing all three magnetic field components at  $r = R_\odot$  we can say nothing for sure about what this magnetic field should look like in the space above the photosphere in reality, i.e. which of the equations should be used to compute the full spatial distribution of  $\vec{B}$ . Thus, Eq. (1) is basic if a magneto-hydrostatic equilibrium and non force-free magnetic field are assumed, and if the plasma pressure and temperature/density distributions are initially known; Eq. (19) is used if a low  $\beta$  approximation, i.e. a force-free magnetic field, is assumed; Equation  $\nabla \times \vec{B} = 0$  if the force-free field is further taken to be potential. Consequently, some decision has to be made on the choice of the most suitable and physically justified equation for computations of  $\vec{B}$  in the corona where  $1 \gg \beta$ . For this reason, the assumption of a force-free magnetic field seems often reasonable for the corona (Gary 2001) and we can integrate Eq. (19) in spherical coordinates along the radial  $r$ -direction starting from the boundary values at  $r = R_\odot$ . The equation Eq. (19) for MHS is now

$$\nabla \times \vec{B} = \alpha \vec{B} \quad \text{with} \quad \alpha = \alpha(r, \theta, \phi) \quad (37)$$

and can be cast in the following set of three scalar equations:

$$\begin{aligned} \alpha &= \frac{1}{r \sin \theta B_r} \left( \cos \theta B_\phi + \right. \\ &\quad \left. + \sin \theta \frac{\partial B_\phi}{\partial \theta} - \frac{\partial B_\theta}{\partial \phi} \right), \\ \frac{\partial B_\phi}{\partial r} &= \frac{1}{r \sin \theta} \left( \frac{\partial B_r}{\partial \phi} + \right. \\ &\quad \left. - \sin \theta B_\phi - \alpha r \sin \theta B_\theta \right), \\ \frac{\partial B_\theta}{\partial r} &= \frac{1}{r} \left( \frac{\partial B_r}{\partial \theta} + \alpha r B_\phi - B_\theta \right). \end{aligned} \quad (38)$$

In addition to Eq. (38), there is also the Gauss law  $\nabla \cdot \vec{B} = 0$  which reduces to

$$\begin{aligned} \frac{\partial B_r}{\partial r} &= -\frac{1}{r \sin \theta} \left( \sin \theta B_r + \cos \theta B_\theta \right. \\ &\quad \left. + \sin \theta \frac{\partial B_\theta}{\partial \theta} + \frac{\partial B_\phi}{\partial \phi} \right). \end{aligned} \quad (39)$$

Eqs. (38) and (39) give the scalar function  $\alpha$  and the  $r$ -derivatives of all three magnetic field components expressed in terms of magnetic field components and their horizontal derivatives at each  $r$ . In the presented form, these equations can easily be integrated numerically in the radial direction starting from  $r = R_\odot$  by applying the procedure as follows.

We start from the photospheric boundary condition with known functional dependences  $B_{r,\theta,\phi}(R_\odot, \theta, \phi)$ . This allows for an immediate computation first of their horizontal  $\theta$ - and  $\phi$ -derivatives, and then the radial  $r$ -derivatives and the scalar function  $\alpha$  by means of Eqs. (38) and (39). Eventually, all three magnetic field components, their three spatial derivatives and the coefficient  $\alpha$  are known at the initial level  $r = R_\odot$ . It should be pointed out that this procedure excludes any arbitrariness regarding the scalar coefficient function  $\alpha$  as it is computed from the first of equations (38) and it depends of the observed magnetic field. A 3D plot of  $\alpha = \alpha(R_\odot, \theta, \phi)$  reveals domains with electric currents where  $\alpha \neq 0$  and possibly also some current-free domains where  $\alpha = 0$  and the magnetic field is potential.

Going to the next level  $r = R_\odot + \delta r$  can now be simply done through the Taylor expansion formula:

$$\begin{aligned} & B_{r,\theta,\phi}(R_\odot + \delta r, \theta, \phi) \\ &= B_{r,\theta,\phi}(R_\odot, \theta, \phi) + \delta r \frac{\partial}{\partial r} B_{r,\theta,\phi} \Big|_{r=R_\odot} \end{aligned} \quad (40)$$

which yields horizontal distribution of magnetic field components at  $r = R_\odot + \delta r$ .

The described procedure is then repeated for each additional step  $\delta r$  in the radial direction giving finally the magnetic field components and the coefficient function  $\alpha$  in the whole domain of the 3D-space. This method however has its technical and physical drawbacks if observed coronal structures are to be recovered: the convergence of the numerical scheme causes problems, and the lack of knowledge on data and effects arising from the magnetic field existing outside the limits of the domain where the boundary values of the observed magnetic field are determined from vector magnetograph data. One can also argue whether the low  $\beta$  condition is really valid at lower corona, chromosphere and photosphere (Gary 2001), i.e. whether Eq. (37) can be fully used to begin with.

Clegg et al. (1999) studied the above problem numerically assuming  $\alpha = \text{const.}$  but had to introduce a global magnetic helicity to obtain magnetic fields over the entire corona and to simulate a particular coronal hole event. Valori et al. (2005) applied a special stress-and-relax computational method for extrapolation of a nonlinear force-free coronal magnetic field (with  $\alpha = \alpha(x, y, z)$ ) from photospheric vector magnetograms.

## 6. CONCLUSIONS

The described procedures of modeling coronal magnetic field topologies are not meant to be fully applicable in recovering particular magnetic structures observed in the corona. They are only supposed to be useful primarily in understanding how complex magnetic structures evolve from various combinations of elementary active regions with sources/sinks of magnetic field at the photospheric level. Similarly to Hoeksema and Scherrer (1986) who computed coronal potential magnetic fields parallel with

photospheric magnetic field observations and for a period of ten years.

In any case, procedures of a proper extrapolation of photospheric magnetic fields into the corona and full reconstruction of total coronal magnetic field topologies related to observed features are still far from being operating well in a general way.

*Acknowledgements* – This work has been carried out within the project "Solar spectral irradiance variation" (No. 1951) supported by the Ministry of Science and Environmental Protection of the Republic of Serbia

## REFERENCES

- Altschuler, M. and Newkirk, G.: 1969, *Solar Phys.*, **9**, 131.
- Aly, J. J. and Seehafer, N.: 1993, *Solar Phys.*, **144**, 243.
- Aly, J. J.: 1992, *Solar Phys.*, **138**, 133.
- Amari, T., Luciani, J. F. and Mikic, Z.: 1999, *Plasma Phys. Control Fusion*, **41**, A779.
- Clegg, J. R., Bromage, J. I. and Browning, P. K.: 1999, *Space Sci. Rev.*, **87**, 145.
- Čadež, V. M. and Ballester, J. L.: 1994, *Astron. Astrophys.*, **292**, 669.
- Čadež, V. M., Ballester, J. L. and Oliver, R.: 1994, *Astron. Astrophys.*, **282**, 934.
- Čadež, V. M.: 1996, *Hvar Obs. Bull.*, **20**, 1.
- Čadež, V. M., Debosscher, A., Messerotti, M., Zlobec, P., Iurcev, I. and Santin, A.: 2005, *Solar Magn. Phenomena*, Springer, Eds. A. Hanselmeier et al. 279
- Edenstrasser, J. W.: 1980, *J. Plasma Physics* **24**, 299.
- Gery, G. A.: 2001, *Solar Phys.*, **203**, 71.
- Hoeksema, J. T. and Scherrer, P. H.: 1986, *Solar Phys.*, **105**, 205.
- Jiao, L., McClymont, A. N. and Mikic, Z.: 1997, *Solar Phys.*, **174** 311.
- Lee, J., White, S. M., Kundu, M. R., Mikic, Z. and McClymont, A. N.: 1999, *Astrophys. J.*, **510**, 413.
- Levine, R. H. and Altschuler, M.: 1974, *Solar Phys.*, **36**, 345.
- Lothian, R.M. and Browning, P.K.: 1995, *Solar Phys.*, **161**, 289.
- Oliver, R., Čadež, V. M. and Ballester, J. L.: 1998 *Astrophys. Space Sci.*, **254**, 67.
- Oliver, R., Čadež, V. M., Carbonell, M. and Ballester, J. L.: 1999 *Astron. Astrophys.*, **351**, 733.
- Petrie, G. J. D. and Neukirch, T.: 2000, *Astron. Astrophys.*, **356**, 735.
- Régnier, S., Amari, T. and Kerselé, E.: 2002, *Astron. Astrophys.*, **392**, 1119.
- Sakurai, T.: 1995, *Space Sci. Rev.*, **51**, 11.
- Valori, G., Kliem, B. and Keppens, R.: 2005, *Astron. Astrophys.*, **433**, 335.
- Yan, Y.: 2003, *Solar Phys.*, **107**, 119.
- Yan, Y. and Sakurai, T.: 2000, *Solar Phys.*, **195**, 89.

- Yan, Y. and Wang, J.: 1995, *Astron. Astrophys.*, **298**, 277.  
Wang, H., Yan, Y., Sakurai, T. and Zhang, M.: 2000, *Solar Phys.*, **197**, 263.  
Wiegelmann, T. and Inhester, B.: 2003, *Solar Phys.*, **214**, 287.  
Wiegelmann, T. and Inhester, B.: 2005, submitted *Solar Phys.*

**МОДЕЛИРАЊЕ СТАТИЧКИХ СТРУКТУРА  
МАГНЕТНИХ ПОЉА У СУНЧЕВОЈ КОРОНИ**

V. M. Čadež

*Astronomical Observatory, Volgina 7, 11160 Belgrade 74, Serbia and Montenegro*

UDK 523.947–337  
*Прегледни рад по позиву*

Даје се преглед разних метода одређивања магнетних поља у сунчевој корони при заданим граничним условима на фотосфери. Посебно се разматра случај магнетних структура које су инваријантне у односу на једну од две хоризонталне координате у Декартовом координатном систему. У том случају могућа

су аналитичка решења којима се могу моделирати бројне сложене структуре полазећи од суперпозиције граничних услова за појединачна локализована елементарна активна подручја са магнетним пољем чије линије сила или извиру или пониру из короне у фотосферу.